Int. J. Solids Structures Vol. 27, No. 2, pp. 189–203, 1991
Printed in Great Britain.

0020–7683/91 $3.00 + .00

A RAYLEIGH–RITZ APPROACH TO TRANSVERSE VIBRATION OF ISOTROPIC AND ANISOTROPIC TRAPEZOIDAL PLATES USING ORTHOGONAL PLATE FUNCTIONS

K. M. LIEW and K. Y. LAM
Department of Mechanical and Production Engineering, National University of Singapore, 10 Kent Ridge Crescent, Singapore 0511, Republic of Singapore

(*Received* 10 *July* 1989; *in revised form* 28 *December* 1989)

Abstract—To overcome the lack of a more general method for free vibration analysis of trapezoidal plates, a computationally efficient and highly accurate Rayleigh–Ritz approach with the newly-developed orthogonal plate functions is proposed to solve these problems with any combination of clamped, simply-supported and free edge support conditions. The deflection of the plate is approximated by a set of two-dimensional orthogonal plate functions, generated using the Gram–Schmidt procedure, which expresses the entire plate domain into two implicitly related variables. In the present paper, the effects of the fibre orientation on the vibrational behaviour of the plates are considered. The numerical results for isotropic and anisotropic trapezoidal plates are presented. Where possible, the numerical results are verified with other existing values in the literature.

NOTATION

a	side of plate
c	height of plate
C_i	coefficient
D	flexural rigidity $= Eh^3/12(1-\nu^2)$
D_{ij}	bending and twisting rigidities of orthotropic plate
E_1, E_2	Young's moduli parallel and perpendicular to the fibres
$f(\xi,\eta)$	generating function
G	shear modulus of elasticity
G_{ij}	shear modulus of elasticity
h	thickness of plate
m	number of terms
M_ξ, M_η	bending moment perpendicular to ξ and η axes
$M_{\xi\eta}$	twisting moment perpendicular to ξ axis
M_n, M_{nt}	bending and twisting moment perpendicular to n direction
n_ξ	$\cos\theta$
n_η	$\sin\theta$
Q_ξ, Q_η	shear force perpendicular to ξ and η axes
Q_n	shear force perpendicular to n direction
T_{max}	maximum kinetic energy
U_{max}	maximum strain energy
$W(\xi,\eta)$	deflection function
x, y	Cartesian coordinates
δ_{ij}	Kronecker delta function
$\varepsilon(\xi,\eta)$	weighting function
$\phi(\xi,\eta)$	orthogonal plate function
ψ_{ij}	coefficient
ξ	x/a
η	y/c
$\sqrt{\lambda^2}$	nondimensional frequency parameter
ν, ν_{12}, ν_{21}	Poisson's ratio
$\varphi(\xi,\eta)$	edge's function
ω	angular frequency of vibration
Π	product of terms
β	angle of fibre orientation
$\lceil x \rceil$	greatest integer function.

1. INTRODUCTION

Excellent reviews of Leissa (1969, 1977, 1981) show that extensive studies have been carried out on the free vibration of rectangular plates; however, very little has been accomplished on plates with other geometrical shapes. In particular, there is little information available for trapezoidal plates. This may be due to the difficulty in forming a simple and adequate deflection function which can apply to the entire plate domain and satisfy the boundary conditions. More research work is needed in this area since such structural elements are commonly encountered in modern technology. The aim of the present paper is to propose a general energy approach using newly developed orthogonal plate functions to solve problems in this area.

Virtually no exact solutions exist for the problem of the trapezoidal plate, not even for the case when all edges are simply-supported. One of the earliest paper by Klein (1955) has reported the fundamental frequency of a simply-supported trapezoidal plate using the collocation method. After that, Chopra and Durvasula (1971, 1972) have investigated the vibration characteristics of simply-supported, symmetric and unsymmetric trapezoidal plates. The Galerkin method is applied with the deflection surface expressed in terms of the Fourier sine series in transformed coordinates. This method is only applicable to plates with simply-supported boundaries. Orris and Petyt (1973) used the finite element method with the quadrilateral plate bending element to obtain frequencies and nodal patterns for completely clamped and simply-supported symmetrical trapezoidal plates. The upper and lower bounds for the first two frequencies of fully-clamped trapezoidal plate were reported by Kuttler and Sigillito (1981). A matrix oriented numerical method has been developed by Srinivasan and Babu (1983) for the analysis of cantilevered quadrilateral plates. Most recently, Saliba (1986, 1988) has adopted the superposition techniques developed by Gorman (1983) to study the free vibration of simply-supported and clamped symmetrical trapezoidal plates.

In previous papers (Liew *et al.*, 1989a, b) a set of two-dimensional orthogonal plate functions was applied to study the free vibration analysis of triangular and rectangular plates. The present paper further extends the potential of the very efficient and highly accurate numerical method to study transverse vibration of trapezoidal plates with different combinations of clamped, simply-supported and free edge support conditions. It is necessary to investigate the vibrational characteristics of trapezoidal plates with different edge support conditions so as to further understand their structural dynamic behaviour and to provide additional design information for this type of plates.

2. DEFLECTION FUNCTION

For convenience, the normalized variables are introduced

$$\xi = x/a; \quad \eta = y/c \tag{1}$$

where x and y are the rectangular coordinates, a is the side of the plate and c is the height of the plate.

The function chosen to represent the deflection $W(\xi, \eta)$ is given by

$$W(\xi, \eta) = \sum_{i=1}^{m} C_i \phi_i(\xi, \eta) \tag{2}$$

where m is the total number of terms, and C_i is the unknown coefficient to be minimized in the Rayleigh–Ritz procedure. The two-dimensional orthogonal plate functions $\phi(\xi, \eta)$ in eqn (2) are generated using the Gram–Schmidt recurrence formula (Liew *et al.*, 1989a, b) and are given as

$$\phi_m(\xi,\eta) = f_m(\xi,\eta)\phi_1(\xi,\eta) - \sum_{i=1}^{m-1} \psi_{m,i}\phi_i(\xi,\eta); \quad m > 1. \tag{3}$$

The generating functions $f_m(\xi, \eta)$, as seen in eqn (3), are chosen to ensure that the higher order members in the set of orthogonal plate functions satisfy the geometrical boundary conditions and to reach faster convergence for the solutions. These generating functions $f_m(\xi, \eta)$ are determined by the following steps:

Let

$$r = \lceil \sqrt{m-1} \rceil \tag{4}$$

$$t = (m-1) - r^2. \tag{5}$$

If t is even, then

$$s = t/2; \quad 0 \leqslant s \leqslant r \tag{6}$$

$$f_m(\xi,\eta) = \xi^r \eta^s. \tag{7}$$

If t is odd, then

$$s = (t-1)/2; \quad 0 \leqslant s \leqslant r-1 \tag{8}$$

$$f_m(\xi,\eta) = \xi^s \eta^r. \tag{9}$$

$\lceil \ \rceil$ in eqn (4) denotes the greatest integer function.

The coefficient $\psi_{m,i}$ in eqn (3) are obtained by multiplying appropriate orthogonal plate functions $\phi_i(\xi, \eta)$ by both sides of eqn (3) and making use of the orthogonality condition,

$$\iint \varepsilon(\xi,\eta)\phi_i(\xi,\eta)\phi_j(\xi,\eta)\,\mathrm{d}\xi\,\mathrm{d}\eta = \delta_{ij}. \tag{10}$$

The coefficients $\psi_{m,i}$ in eqn (3) become

$$\psi_{m,i} = \frac{\iint f_m(\xi,\eta)\varepsilon(\xi,\eta)\phi_1(\xi,\eta)\phi_i(\xi,\eta)\,\mathrm{d}\xi\,\mathrm{d}\eta}{\iint \varepsilon(\xi,\eta)\phi_i^2(\xi,\eta)\,\mathrm{d}\xi\,\mathrm{d}\eta}, \tag{11}$$

where δ_{ij} is the Kronecker delta, $\varepsilon(\xi, \eta)$ is the weighting function and the integration is carried out over the entire plate domain. The weighting function is used to account for the thickness variation in the geometry which is taken as unity in the present analysis since plates with only uniform thickness are considered.

The starting function $\phi_1(\xi, \eta)$ mentioned in eqn (3) applied to a trapezoid is given by

$$\phi_1(\xi,\eta) = \prod_{n=1}^{4} \varphi_n(\xi,\eta) \tag{12}$$

where Π denotes the product of terms, n is the number of sides, and $\varphi(\xi, \eta)$ is the edge function which is obtained according to the individual edge support conditions. A detailed procedure of forming $\varphi(\xi, \eta)$ is given below:

(a) for simply-supported edge

$$\varphi(\xi,\eta)=\begin{cases}\xi-a & \text{at edge } \xi=a\\ \eta-c & \text{at edge } \eta=c\\ \eta-m\xi-d & \text{at edge } \eta=m\xi+d\end{cases} \tag{13}$$

(b) for clamped edge

$$\varphi(\xi,\eta)=\begin{cases}(\xi-a)^2 & \text{at edge } \xi=a\\ (\eta-c)^2 & \text{at edge } \eta=c\\ (\eta-m\xi-d)^2 & \text{at edge } \eta=m\xi+d \quad \text{and}\end{cases} \tag{14}$$

(c) for free edge

$$\varphi(\xi,\eta)=1. \tag{15}$$

3. BOUNDARY CONDITIONS

The starting function $\phi_1(\xi,\eta)$ is chosen to satisfy at least the geometrical boundary conditions of the plate. Better convergence is achieved if $\phi_1(\xi,\eta)$ also satisfies the natural boundary conditions. The geometrical boundary conditions and natural boundary conditions for different support edges are given as follows (Timoshenko, 1970):

(a) for simply-supported edge

$$\phi_1(\xi,\eta)=0 \tag{16}$$

$$M_n=M_\xi n_\xi^2-2M_{\xi\eta}n_\xi n_\eta+M_\eta n_\eta^2=0 \tag{17}$$

where

$$n_\xi=\cos\theta \tag{18}$$

$$n_\eta=\sin\theta, \tag{19}$$

(b) for clamped edge

$$\phi_1(\xi,\eta)=0 \tag{20}$$

$$\frac{\partial\phi_1(\xi,\eta)}{\partial n}=n_\xi\frac{\partial\phi_1(\xi,\eta)}{\partial\xi}+n_\eta\frac{\partial\phi_1(\xi,\eta)}{\partial\eta}=0 \quad \text{and} \tag{21}$$

(c) for free edge

$$M_n=0 \tag{22}$$

$$V_n=Q_n-\frac{\partial M_{nt}}{\partial s}=0 \tag{23}$$

where

$$Q_n=Q_\xi n_\xi+Q_\eta n_\eta \tag{24}$$

$$M_{nt}=M_{\xi\eta}(n_\xi^2-n_\eta^2)+(M_\xi-M_\eta)n_\xi n_\eta. \tag{25}$$

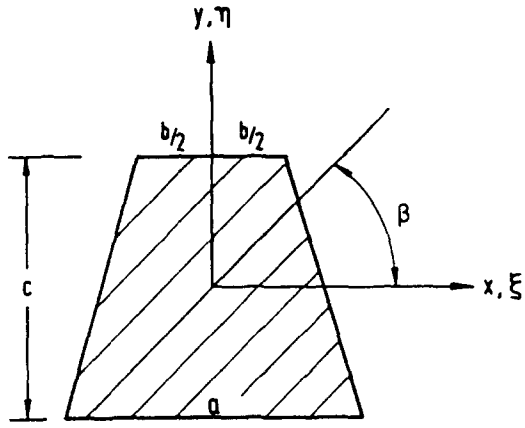

Fig. 1. Geometry of trapezoidal plate.

4. METHOD OF ANALYSIS

The approximate solutions for free vibration of a thin trapezoidal plate, shown in Fig. 1, can be derived using Rayleigh's principle. The maximum strain and kinetic energies of the anisotropic plate are given by

$$U_{max} = \tfrac{1}{2}ac\int\int\left\{\frac{D_{11}}{a^4}\left(\frac{\partial^2 W}{\partial\xi^2}\right)^2 + \frac{2D_{12}}{a^2c^2}\left(\frac{\partial^2 W}{\partial\xi^2}\frac{\partial^2 W}{\partial\eta^2}\right) + \frac{D_{22}}{c^4}\left(\frac{\partial^2 W}{\partial\eta^2}\right)^2 + \frac{4D_{66}}{a^2c^2}\left(\frac{\partial^2 W}{\partial\xi\partial\eta}\right)^2 + \frac{4D_{16}}{a^3c}\left(\frac{\partial^2 W}{\partial\xi^2}\frac{\partial^2 W}{\partial\xi\partial\eta}\right) + \frac{4D_{26}}{ac^3}\left(\frac{\partial^2 W}{\partial\eta^2}\frac{\partial^2 W}{\partial\xi\partial\eta}\right)\right\} d\xi\, d\eta \quad (26)$$

and

$$T_{max} = \tfrac{1}{2}\rho hac\omega^2\int\int W^2(\xi,\eta)\, d\xi\, d\eta \quad (27)$$

where ρ is the material density, h is the plate thickness and ω is the angular frequency of vibration.

The bending stiffnesses D_{ij} of the plate can be expressed in terms of the orthotropic elastic constants Q_{ij} along the principal axis of orthotropy as follows:

$$D_{11} = Q_{11}\cos^4\beta + 2(Q_{12}+2Q_{66})\sin^2\beta\cos^2\beta + Q_{22}\sin^4\beta \quad (28)$$

$$D_{22} = Q_{11}\sin^4\beta + 2(Q_{12}+2Q_{66})\sin^2\beta\cos^2\beta + Q_{22}\cos^4\beta \quad (29)$$

$$D_{12} = (Q_{11}+Q_{22}-4Q_{66})\sin^2\beta\cos^2\beta + Q_{12}(\sin^4\beta+\cos^4\beta) \quad (30)$$

$$D_{16} = (Q_{11}-Q_{12}-2Q_{66}\sin\beta\cos^3\beta + (Q_{12}-Q_{22}+2Q_{66})\sin^3\beta\cos\beta \quad (31)$$

$$D_{26} = (Q_{11}-Q_{12}-2Q_{66})\sin^3\beta\cos\beta + (Q_{12}-Q_{22}+2Q_{66})\sin\beta\cos^3\beta \quad (32)$$

$$D_{66} = (Q_{11}+Q_{22}-2Q_{12}-2Q_{66})\sin^2\beta\cos^2\beta + Q_{66}(\sin^4\beta+\cos^4\beta) \quad (33)$$

where

$$Q_{11} = \frac{E_1 h^3}{12(1-\nu_{12}\nu_{21})} \tag{34}$$

$$Q_{12} = \frac{\nu_{12} E_2 h^3}{12(1-\nu_{12}\nu_{21})} \tag{35}$$

$$Q_{22} = \frac{E_2 h^3}{12(1-\nu_{12}\nu_{21})} \tag{36}$$

$$Q_{66} = \frac{G_{12} h^3}{12} \tag{37}$$

$$\nu_{12} E_1 = \nu_{12} E_2, \tag{38}$$

in which β is the angle of fibre orientation with respect to the ξ axis shown in Fig. 1, E_1 and E_2 are the Young's moduli parallel and perpendicular to the fibres respectively, ν_{12} and ν_{21} are the corresponding Poisson's ratios, and G_{12} is the shear modulus of elasticity.

Substituting eqn (2) into eqns (26) and (27) and minizing the Rayleigh quotient with respect to the undetermined coefficients C_i

$$\frac{\partial}{\partial C_i}\iint\left\{\frac{D_{11}}{a^4}\left[\frac{\partial^2\sum_{i=1}^{m} C_i\phi_i(\xi,\eta)}{\partial\xi^2}\right]^2 + \frac{2D_{12}}{a^2c^2}\left[\frac{\partial^2\sum_{i=1}^{m} C_i\phi_i(\xi,\eta)}{\partial\xi^2}\,\frac{\partial^2\sum_{i=1}^{m} C_i\phi_i(\xi,\eta)}{\partial\eta^2}\right]\right.$$

$$+\frac{D_{22}}{c^4}\left[\frac{\partial^2\sum_{i=1}^{m} C_i\phi_i(\xi,\eta)}{\partial\eta^2}\right]^2 + \frac{4D_{66}}{a^2c^2}\left[\frac{\partial^2\sum_{i=1}^{m} C_i\phi_i(\xi,\eta)}{\partial\xi\partial\eta}\right]^2$$

$$+\frac{4D_{16}}{a^3c}\left[\frac{\partial^2\sum_{i=1}^{m} C_i\phi_i(\xi,\eta)}{\partial\xi^2}\,\frac{\partial^2\sum_{i=1}^{m} C_i\phi_i(\xi,\eta)}{\partial\xi\partial\eta}\right]$$

$$\left.+\frac{4D_{26}}{ac^3}\left[\frac{\partial^2\sum_{i=1}^{m} C_i\phi_i(\xi,\eta)}{\partial\eta^2}\,\frac{\partial^2\sum_{i=1}^{m} C_i\phi_i(\xi,\eta)}{\partial\xi\partial\eta}\right]\right\}\mathrm{d}\xi\,\mathrm{d}\eta$$

$$-\frac{\partial}{\partial C_i}\left[\rho h\omega^2\iint\sum_{i=1}^{m} C_i\phi_i(\xi,\eta)\,\mathrm{d}\xi\,\mathrm{d}\eta\right] = 0, \tag{39}$$

leads to the governing eigenvalue equation

$$\sum[K_{ij} - \lambda M_{ij}]C_i = 0 \tag{40}$$

where

$$K_{ij} = \frac{1}{\sqrt{D_{11}D_{22}}}[D_{11}P_{ij} + \alpha^4 D_{22}Q_{ij} + 2\alpha^2 D_{12}(R_{ij}+S_{ij})$$

$$+4\alpha^2 D_{66}T_{ij} + 2\alpha D_{16}(U_{ij}+V_{ij}) + 2\alpha^3 D_{26}(W_{ij}+X_{ij})] \tag{41}$$

$$\lambda = \frac{\rho h\omega^2 a^4}{\sqrt{D_{11}D_{22}}}; \quad \alpha = a/c \tag{42}$$

$$M_{ij} = \int\int \phi_i(\xi,\eta)\phi_j(\xi,\eta)\,d\xi\,d\eta \tag{43}$$

$$P_{ij} = \int\int \frac{\partial^2\phi_i(\xi,\eta)}{\partial\xi^2}\frac{\partial^2\phi_j(\xi,\eta)}{\partial\xi^2}\,d\xi\,d\eta \tag{44}$$

$$Q_{ij} = \int\int \frac{\partial^2\phi_i(\xi,\eta)}{\partial\eta^2}\frac{\partial^2\phi_j(\xi,\eta)}{\partial\eta^2}\,d\xi\,d\eta \tag{45}$$

$$R_{ij} = \int\int \frac{\partial^2\phi_i(\xi,\eta)}{\partial\eta^2}\frac{\partial^2\phi_j(\xi,\eta)}{\partial\xi^2}\,d\xi\,d\eta \tag{46}$$

$$S_{ij} = \int\int \frac{\partial^2\phi_i(\xi,\eta)}{\partial\xi^2}\frac{\partial^2\phi_j(\xi,\eta)}{\partial\eta^2}\,d\xi\,d\eta \tag{47}$$

$$T_{ij} = \int\int \frac{\partial^2\phi_i(\xi,\eta)}{\partial\xi\partial\eta}\frac{\partial^2\phi_j(\xi,\eta)}{\partial\xi\partial\eta}\,d\xi\,d\eta \tag{48}$$

$$U_{ij} = \int\int \frac{\partial^2\phi_i(\xi,\eta)}{\partial\xi^2}\frac{\partial^2\phi_j(\xi,\eta)}{\partial\xi\partial\eta}\,d\xi\,d\eta \tag{49}$$

$$V_{ij} = \int\int \frac{\partial^2\phi_i(\xi,\eta)}{\partial\xi\partial\eta}\frac{\partial^2\phi_j(\xi,\eta)}{\partial\xi^2}\,d\xi\,d\eta \tag{50}$$

$$W_{ij} = \int\int \frac{\partial^2\phi_i(\xi,\eta)}{\partial\eta^2}\frac{\partial^2\phi_j(\xi,\eta)}{\partial\xi\partial\eta}\,d\xi\,d\eta \tag{51}$$

$$X_{ij} = \int\int \frac{\partial^2\phi_i(\xi,\eta)}{\partial\xi\partial\eta}\frac{\partial^2\phi_j(\xi,\eta)}{\partial\eta^2}\,d\xi\,d\eta. \tag{52}$$

Equation (40) yields an eigenvalue determinant, the zeros of which give the natural frequencies of the plate. Back substitution yields the coefficient vectors; substitution of these coefficient vectors into eqn (2) gives the mode shapes of the plate.

5. RESULTS AND DISCUSSION

The numerical calculations for the natural frequencies using the proposed method are carried out for six different combinations of edge supported trapezoidal plates, namely:

(i) four edges simply-supported (S–S–S–S),
(ii) four edges fully-clamped (C–C–C–C),
(iii) one edge clamped and three edges simply-supported (C–S–S–S),
(iv) two opposite edges clamped and the other two simply-supported (C–S–C–S),
(v) cantilevered (C–F–F–F) and
(vi) one edge clamped, two opposite edges simply-supported and one edge free (C–S–F–S).

The symbolism C–S–F–S, for example, identifies a trapezoidal plate with edges clamped, simply-supported, free and simply-supported; start counting anticlockwise from the base of the trapezoidal plate. The stiffness properties for the boron–epoxy are given in

Table 1. Material properties of unidirectional composite

Material	Major elastic modulus, E_1 (GPa)	Minor elastic modulus, E_2 (GPa)	Shear modulus G_{12} (GPa)	Major Poisson's ratio, ν_{12}
Isotropic	1.0	1.0	0.385	0.30
Boron–epoxy	204	18.50	5.59	0.23

Table 1. The obtained natural frequencies for the anisotropic plate are expressed in terms of the nondimensional frequency parameters $\sqrt{\lambda'}$:

$$\sqrt{\lambda'} = \frac{\omega a^2}{2\pi}\sqrt{\frac{\rho h}{(D_{11}D_{22})^{1/2}}}. \tag{53}$$

The anisotropic case can be simplified to isotropic case by setting

$$\nu_{12} = \nu_{21} = 0.30 \tag{54}$$

$$D_{11} = D_{22} = D = \frac{Eh^3}{12(1-\nu)^2} \tag{55}$$

$$D_{66} = \tfrac{1}{2}(1-\nu)D \tag{56}$$

and the nondimensional frequency parameter $\sqrt{\lambda'}$ becomes

$$\sqrt{\lambda'} = \frac{\omega a^2}{2\pi}\sqrt{\rho h/D}. \tag{57}$$

5.1. *Convergence of solution*

The Rayleigh–Ritz energy approach gives an upper-bound solution to the exact value. A convergence study is carried out so as to ensure that the solutions to the problem are convergent and to establish the optimum number of terms required in the deflection function in order to obtain satisfactory results.

Tables 2 and 3 are the convergence patterns of the first four nondimensional frequency parameters for the simply-supported and fully-clamped isotropic trapezoidal plates with ratio $b/a = 1/5$ and $3/5$, respectively. It can be observed from the Tables 2 and 3 that it is sufficient to take $m = 20$ to reach stable convergence since $m = 24$ produces no drastic change in the solutions compared with that obtained with $m = 20$.

The convergence patterns of the fundamental nondimensional frequency parameters for the simply-supported and fully-clamped anisotropic trapezoidal plates are given in Tables 4 and 5. The fundamental nondimensional frequency parameters are studied by

Table 2. Convergence pattern of the nondimensional frequency parameter $\sqrt{\lambda'} = (\omega a^2/2\pi)(\rho h/D)^{1/2}$ of a simply-supported isotropic trapezoidal plate ($a/c = 1.0$)

b/a	Mode no.	Number of terms, m					
		4	8	12	16	20	24
1/5	1	6.67	6.02	6.02	6.01	6.01	6.01
	2	20.01	13.03	12.83	12.73	12.71	12.69
	3	20.19	19.08	15.48	15.46	15.34	15.34
	4	37.64	35.77	22.63	22.53	21.82	21.73
3/5	1	4.34	4.09	4.09	4.08	4.08	4.08
	2	11.95	9.42	9.01	8.94	8.93	8.91
	3	13.75	13.52	11.19	11.17	11.12	11.12
	4	21.36	20.08	17.67	16.93	16.76	16.72

Table 3. Convergence pattern of the nondimensional frequency parameter $\sqrt{\lambda} = (\omega a^2/2\pi)(\rho h/D)^{1/2}$ of a fully-clamped isotropic trapezoidal plate ($a/c = 1.0$)

b/a	Mode no.	Number of terms, m					
		4	8	12	16	20	24
1.5	1	11.48	11.33	11.33	11.33	11.32	11.32
	2	24.18	19.92	19.46	19.45	19.45	19.45
	3	25.55	23.99	23.32	23.31	23.30	23.30
	4	39.84	37.94	32.21	30.70	30.59	30.57
3.5	1	7.62	7.57	7.56	7.55	7.55	7.55
	2	15.34	13.44	13.35	13.35	13.34	13.34
	3	16.98	16.98	16.71	16.71	16.70	16.70
	4	24.39	23.55	22.58	22.56	22.44	22.42

Table 4. Convergence pattern of the fundamental nondimensional frequency parameter $\sqrt{\lambda} = (\omega a^2/2\pi)(\rho h/\sqrt{D_{11}D_{12}})^{1/2}$ of a simply-supported boron–epoxy trapezoidal plate ($a/c = 1.0$)

h/a	Angle β°	Number of terms, m				
		4	8	12	16	20
1/5	0	6.46	5.61	5.56	5.51	5.51
	15	6.82	5.89	5.85	5.81	5.80
	30	7.60	6.64	6.62	6.60	6.59
	45	8.24	7.32	7.31	7.30	7.30
3/5	0	3.79	3.63	3.62	3.61	3.61
	15	4.24	4.06	4.05	4.05	4.04
	30	5.09	4.85	4.83	4.83	4.83
	45	5.64	5.34	5.33	5.33	5.33

Table 5. Convergence pattern of the fundamental nondimensional frequency parameter $\sqrt{\lambda} = (\omega a^2/2\pi)(\rho h/\sqrt{D_{11}D_{12}})^{1/2}$ of a fully-clamped boron–epoxy trapezoidal plate ($a/c = 1.0$)

h/a	Angle β°	Number of terms, m				
		4	8	12	16	20
1/5	0	12.26	10.45	9.72	9.43	9.43
	15	12.48	10.95	10.42	10.22	10.22
	30	13.02	12.15	11.99	11.93	11.93
	45	13.58	13.30	13.30	13.29	13.29
3/5	0	7.59	7.51	7.48	7.47	7.47
	15	7.91	7.68	7.65	7.64	7.64
	30	8.35	8.15	8.12	8.11	8.11
	45	8.94	8.84	8.82	8.81	8.81

varying the number of terms m for different ratio $b/a = 1/5$ and $3/5$. The study shows that stable and convergent results are obtained when $m = 16$ is used.

To optimize the usage of computational time and to obtain satisfactory results, $m = 20$ is used for the isotropic cases to calculate the first four nondimensional frequency parameters and $m = 16$ is used for the anisotropic cases to compute the fundamental nondimensional frequency parameters.

5.2. *Numerical results*

The nondimensional frequency parameters of the simply-supported isotropic trapezoidal plate with different b/a ratio are given in Table 6. The ratio $b/a = 0$ is corresponding to an isosceles triangular plate and $b/a = 1$ is a square plate. The present results are compared with the values of Chopra and Durvasula (1971). Close agreement is seen to exist between the present results and those of the Chopra and Durvasula (1971).

Table 6. Comparison of the nondimensional frequency parameter $\sqrt{\lambda'} = (\omega a^2 2\pi)(\rho h/D)^{1/2}$ of a simply-supported isotropic trapezoidal plate ($a/c = 1.0$)

b/a	Reference	Mode numbers 1	2	3	4
0	Chopra	7.30	16.37	17.69	28.26
	Present	7.30	16.32	17.64	28.43
1/5	Chopra	6.01	12.68	15.38	21.46
	Present	6.01	12.69	15.34	21.73
2/5	Chopra	4.90	10.17	13.19	18.05
	Present	4.90	10.24	13.17	17.72
3/5	Chopra	4.08	8.91	11.14	16.74
	Present	4.08	8.91	11.12	16.72
4/5	Chopra	3.52	8.24	9.31	14.16
	Present	3.52	8.24	9.29	14.20
1.0	Chopra	3.14	7.85	7.85	12.57
	Present	3.14	7.84	7.84	12.59

The second set of results available for the comparison is the case for fully-clamped isotropic trapezoidal plate. The nondimensional frequency parameters of the fully-clamped trapezoidal plate together with the upper and lower bound solutions of Kuttler and Sigillito (1981) are tabulated in Table 7. Since only the first two frequencies are published by Kuttler and Sigillito, the present results are compared with these two values. The comparison shows that the present solutions are within the upper and lower bound solutions of Kuttler and Sigillito.

The variation of the nondimensional frequency parameters with different b/a ratios for the C–S–S–S, C–S–C–S, C–F–F–F and C–S–F–S isotropic trapezoidal plates is given in Tables 8–11. It is evident from the tables that the nondimensional frequency parameter decreases with the increase in the b/a ratio. This behavior is expected because with the increase in the b/a ratio, the flexibility of the plate also increases.

To investigate the influence of the fibre orientation on the vibration behaviour of trapezoidal plates, the six examples are again analysed with different fixed ratio b/a. The numerical results are presented graphically for the simply-supported, fully-clamped, C–S–S–S, C–S–C–S, C–F–F–F and C–S–C–F trapezoidal plates with different fibre orientation angle α varying from 0° to 90°.

Table 7. Comparison of the nondimensional frequency parameter $\sqrt{\lambda'} = (\omega a^2/2\pi)(\rho h/D)^{1/2}$ of a fully-clamped isotropic trapezoidal plate ($a/c = 1.0$)

b/a	Reference	Mode numbers 1	2	3	4
0	Kuttler (upper bounds)	13.73	25.41		
	Kuttler (lower bounds)	13.70	25.28		
	Present	13.73	25.40	26.98	39.46
1/5	Kuttler (upper bounds)	11.35	19.93		
	Kuttler (lower bounds)	11.31	19.77		
	Present	11.32	19.45	23.30	30.57
2/5	Kuttler (upper bounds)	9.23	15.63		
	Kuttler (lower bounds)	9.18	15.45		
	Present	9.22	15.59	19.87	24.55
3/5	Kuttler (upper bounds)	7.57	13.39		
	Kuttler (lower bounds)	7.52	13.27		
	Present	7.55	13.34	16.70	22.42
4/5	Kuttler (upper bounds)	6.45	12.30		
	Kuttler (lower bounds)	6.41	12.20		
	Present	6.44	12.27	13.88	19.44
1.0	Kuttler (upper bounds)	5.73	11.10		
	Kuttler (lower bounds)	5.72	11.61		
	Present	5.73	11.68	11.68	17.22

Table 8. The nondimensional frequency parameter $\sqrt{\lambda'} = (\omega a^2/2\pi)(\rho h/D)^{1/2}$ of a C–S–S–S isotropic trapezoidal plate ($a/c = 1.0$)

b/a	Mode numbers 1	2	3	4
0	9.02	18.93	20.21	31.71
1/5	7.26	14.55	17.24	24.14
2/5	5.80	11.72	14.48	20.44
3/5	4.80	10.40	11.94	18.16
4/5	4.16	9.73	9.81	15.34
1.0	3.76	8.21	9.34	13.71

Table 9. The nondimensional frequency parameter $\sqrt{\lambda'} = (\omega a^2/2\pi)(\rho h/D)^{1/2}$ of a C–S–C–S isotropic trapezoidal plate ($a/c = 1.0$)

b/a	Mode numbers 1	2	3	4
0	9.02	18.93	20.21	31.71
1/5	7.30	14.83	17.25	24.72
2/5	6.08	12.76	14.49	22.33
3/5	5.35	11.83	12.04	18.78
4/5	4.90	10.10	11.34	16.44
1.0	4.61	8.70	11.03	15.05

Table 10. The nondimensional frequency parameter $\sqrt{\lambda'} = (\omega a^2/2\pi)(\rho h/D)^{1/2}$ of a C–F–F–F isotropic trapezoidal plate ($a/c = 1.0$)

b/a	Mode numbers 1	2	3	4
0	1.07	4.64	4.65	11.03
1/5	0.82	3.53	3.88	9.20
2/5	0.70	2.66	3.67	7.31
3/5	0.64	2.06	3.56	6.20
4/5	0.59	1.65	3.48	5.46
1.0	0.55	1.36	3.39	4.36

Table 11. The nondimensional frequency parameter $\sqrt{\lambda'} = (\omega a^2/2\pi)(\rho h/D)^{1/2}$ of a C–S–F–S isotropic trapezoidal plate ($a/c = 1.0$)

b/a	Mode numbers 1	2	3	4
0	9.02	18.93	20.21	31.71
1/5	7.23	14.36	17.24	23.14
2/5	5.53	9.83	14.48	15.91
3/5	3.92	7.08	11.83	13.15
4/5	2.75	5.89	9.03	12.11
1.0	2.02	5.27	6.63	10.05

The fundamental frequency parameters for the simply-supported anisotropic plate with different fibre orientation angles β at the fixed b/a ratios are given in Fig. 2. A maximum frequency occurred at $\beta = 45°$ for the isosceles triangular plate ($b/a = 0$). For trapezoidal plates with $b/a = 0.2$ and 0.4, both maximum frequencies occurred at $\beta = 30°$. The maximum frequencies for the trapezoidal plate with b/a in the ranges from 0.6 to 1.0 occurred at $\beta = 45°$.

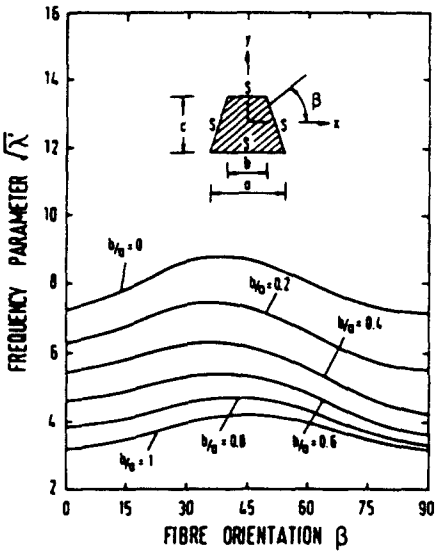

Fig. 2. Variation of frequency parameter with respect to fibre orientation of a simply-supported trapezoidal plate ($a/c = 1.0$).

The variation of the frequency parameters with respect to the fibre orientation of the fully-clamped anisotropic trapezoidal plate is presented in Fig. 3. The maximum frequency for the ratio $b/a = 0$ occurred at $\beta = 45°$. When ratio $b/a = 0.2$ and 0.4, frequencies reach maximum at $\beta = 30°$ and 15°. Further increase in the ratio b/a from 0.4 to 1 and all maximum frequencies are at $\beta = 0°$.

Figure 4 shows the results for the C-S-S-S anisotropic trapezoidal plate. For ratios within the range $0 \leqslant b/a \leqslant 1.0$, maximum frequencies occurred at $\beta = 45°$, except for the ratio $b/a = 1.0$ where the maximum value occurred at $\beta = 60°$.

The variation of the frequency parameters with respect to the fibre orientation of the C-S-C-S anisotropic trapezoidal plate is given in Fig. 5. For the ratio $b/a = 0$–0.2, 0.4, 0.6 and 0.8–1.0, the maximum frequencies occur at $\beta = 45°$, 60°, 75° and 90° which can be seen from the figure.

All maximum frequencies occurred at $\beta = 90°$ for the cantilevered anisotropic trapezoidal plate with fixed ratio b/a as shown in Fig. 6.

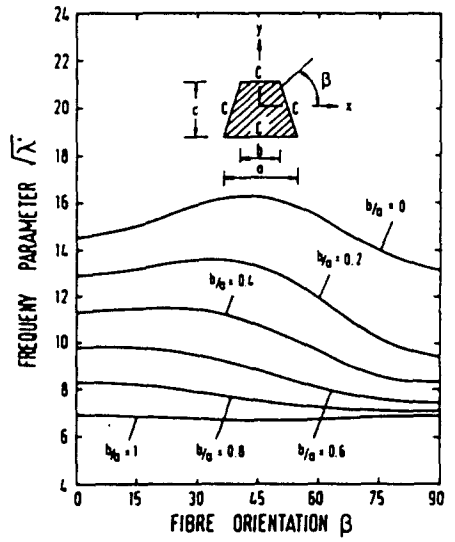

Fig. 3. Variation of frequency parameter with respect to fibre orientation of a fully-clamped trapezoidal plate ($a/c = 1.0$).

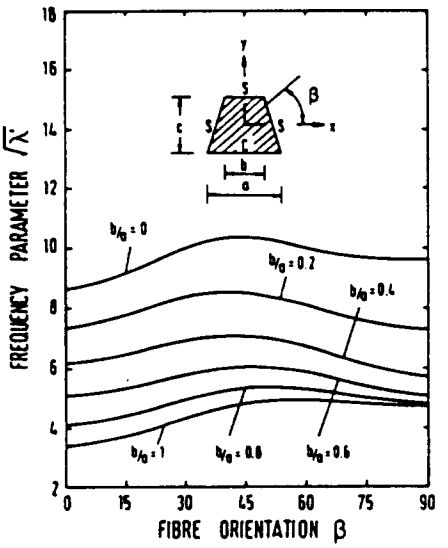

Fig. 4. Variation of frequency parameter with respect to fibre orientation of a C–S–S–S trapezoidal plate (a/c = 1.0).

The results for the C–S–F–S anisotropic trapezoidal plate are given in Fig. 7. For ratio b/a = 0–0.2, 0.4, 0.6 and 0.8–1.0, maximum frequencies occurred at $\beta = 45°$, 30°, 15° and 0° which can be observed from the figure.

It can be concluded from the above investigation that the effect of fibre orientation on the vibration frequency depends on the boundary conditions and the b/a ratio of the plates.

6. CONCLUSION

The paper has presented the free vibration studies of symmetrical isotropic and anisotropic trapezoidal plates. The proposed method adopted the Rayleigh–Ritz energy approach and employed the two-dimensional orthogonal plate functions as the admissible functions to approximate the natural frequency of the trapezoidal plates with different combinations of clamped, simply-supported and free edge support conditions.

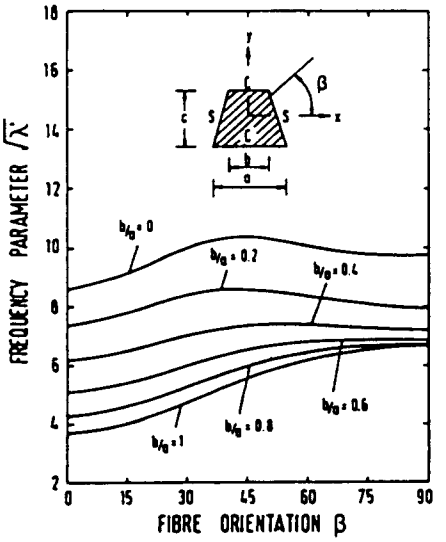

Fig. 5. Variation of frequency parameter with respect to fibre orientation of a C–S–C–S trapezoidal plate (a/c = 1.0).

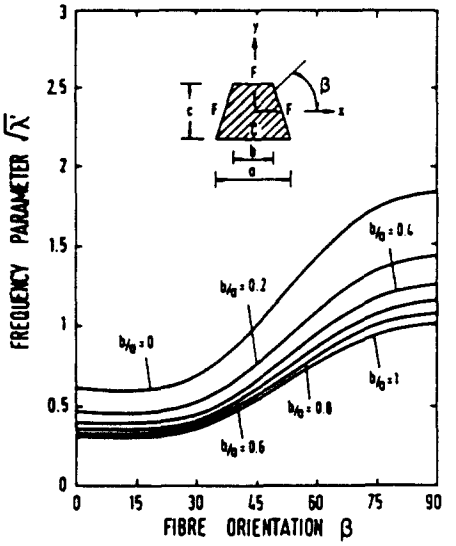

Fig. 6. Variation of frequency parameter with respect to fibre orientation of a cantilevered trapezoidal plate (a/c = 1.0).

Numerical results for six different edge supported trapezoidal plates are presented. These values have been verified with the available literature results for the isotropic simply-supported and fully-clamped trapezoidal plates. No comparison can be made for the isotropic C–S–S–S, C–S–C–S, C–F–F–F and C–S–C–F trapezoidal plates because no results for such cases are available.

To show the effect of the fibre orientation on the vibrational behaviour of the trapezoidal plates, the six plates previous study are again analyzed with different angles of fibre orientation varying from zero to ninety degrees. The study shows that this effect depends on the boundary conditions of the plate and the b/a ratio. This observation is particularly important since composite plates are commonly used in modern technology nowadays. It provides valuable information for researchers and engineers in design applications.

REFERENCES

Chopra, I. and Durvasula, S. (1971). Vibration of simply-supported trapezoidal plates. Part I. Symmetric trapezoids. *J. Sound Vibr.* **19**, 379–392.

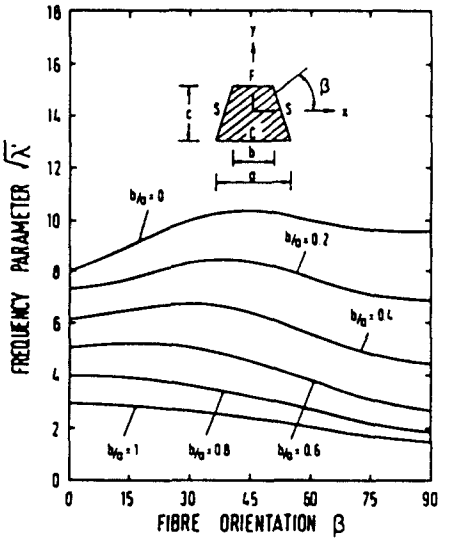

Fig. 7. Variation of frequency parameter with respect to fibre orientation of a C–S–F–S trapezoidal plate (a/c = 1.0).

Chopra, I. and Durvasula, S. (1972). Vibration of simply-supported trapezoidal plates. Part II. Unsymmetric trapezoids. *J. Sound Vibr.* **20**, 125–134.

Gorman, D. J. (1983). Highly accurate analytical solution for free vibration analysis of simply-supported right triangular plates. *J. Sound Vibr.* **89**, 107–118.

Jackson, D. (1936). Formal properties of orthogonal polynomials in two variables. *Duke Math. Jl* **2**, 423–434.

Klein, B. (1955). Vibration of simply supported isosceles trapezoidal flat plates. *J. Acoust. Soc. Am.* **27**, 1059–1060.

Kuttler, J. R. and Sigillito, V. G. (1981). Upper and lower bounds for frequencies of trapezoidal and triangular plates. *J. Sound Vibr.* **78**, 585–590.

Leissa, A. W. (1969). Vibration of plates. NASA SP-160.

Leissa, A. W. (1977). Recent research in plate vibrations: classical theory. *Shock Vibr. Digest* **9**, 13–24.

Leissa, A. W. (1981). Plate vibration research, 1976–1980: classical theory. *Shock Vibr. Digest* **13**, 11–22.

Liew, K. M., Lam, K. Y. and Chow, S. T. (1989a). Study on flexural vibration of triangular composite plates influenced by fibre orientation. *J. Compos. Structures* (in press).

Liew, K. M., Lam, K. Y. and Chow, S. T. (1989b). Free vibration analysis of rectangular plates using orthogonal plate function. *J. Comput. Structures* (in press).

Orris, R. M. and Petyt, M. (1973). A finite element study of the vibration of trapezoidal plates. *J. Sound Vibr.* **27**, 325–344.

Saliba, H. T. (1986). Free vibration analysis of simply-supported symmetrical trapezoidal plates. *J. Sound Vibr.* **110**, 87–97.

Saliba, H. T. (1988). Transverse free vibration of fully clamped symmetrical trapezoidal plates. *J. Sound Vibr.* **126**, 237–247.

Srinivasan, R. S. and Babu, B. J. C. (1983). Free vibration of cantilever quadrilateral plates. *J. Acoust. Soc. Am.* **73**, 851–855.

Timoshenko, S. (1970). *Theory of Plates and Shells*, 2nd Edn. McGraw-Hill, New York.